BIOLOGICAL CHARACTERISATION OF SOMATROPIN-DERIVED CRYPTIC PEPTIDES

Liesa Tack[a,e], Nathalie Bracke[a,e], Frederick Verbeke[a], Evelien Wynendaele[a], Ewald Pauwels[b], Alex Maes[c], Christophe Van de Wiele[c], Mike Sathekge[d], and Bart De Spiegeleer[a,]*

[a] Drug Quality and Registration (DruQuaR) group, Department of Pharmaceutical analysis, Faculty of Pharmaceutical Sciences, Ghent University, Ottergemsesteenweg 460, B-9000 Ghent, Belgium.

[b] Centre for Molecular Modelling, Ghent University, Technologiepark 903, B-9052, Zwijnaarde, Belgium.

[c] AZ Groeninge, Department of Nuclear Medicine, Catholic University Leuven, B-8500 Kortrijk, Belgium.

[d] Department of Nuclear Medicine, Steve Biko Academic Hospital, University of Pretoria, 0002, South Africa.

[e] These authors contributed equally to this work.

(O/Ref. 2018-202)

* Corresponding author:

Tel: + 32 9 264 81 00

Fax: + 32 9 264 81 93

E-mail: bart.despiegeleer@ugent.be

ORCID number: 0000-0001-6794-3108

ACKNOWLEDGMENTS

This research project was supported by grants from the Research Foundation FWO (Flanders) and NRF (South-Africa) (grant number G0G7617N) to Liesa Tack and from the Institute for the Promotion of Innovation through Science and Technology in Flanders (IWT-Vlaanderen) to Frederick Verbeke (Grant 131356). We thank Dr. Ellen

Heyndrickx and Marianne Lauwers (under supervision of Dr. S. De Saeger) for their operational help in the nondenaturing MS experiments using the Waters Synapt G2-Si high-resolution quadrupole time-of-flight mass spectrometer, which use was financially made possible by Hercules (Grant AUGE/13/13), and Bart Jr. De Spiegeleer for his help in the native MS data evaluation using Python programming. We also thank Dr. Neil Charter from Lead Hunter Discovery Services (DiscoverX) for his contribution in the PathHunter bioassay.

ABSTRACT

Little is known about possible cryptic peptides of the recombinant growth hormone (somatropin). In this study, six synthetic somatropin-derived peptides (SDPs) were selected based on their sequences which correspond to the binding interface of the growth hormone receptor. Their novelty was confirmed by *in silico* and *in vitro* proteolytic digestion of somatropin. Chemical characterisation of the SDPs, *i.e.* identification via LC-MS and purity quantification via HPLC-UV and U(H)PLC-MRM, was first performed. All the SDPs were stable in brain tissue homogenate, liver tissue homogenate and serum ($t_{1/2}$ > 15 min). The metabolites in brain and serum, formed between 15 min and 120 min, were also identified. The interactions towards the growth hormone receptor (GHR) and the human growth hormone binding protein (hGHBp) were also evaluated using GHR bioassay and native MS. No interaction was detected under the applied conditions. A last part of the study investigated the pharmacokinetics and tissue distribution of two peptides (*i.e.* $SDP_{167-175}$ and $SDP_{101-121}$), selected based on their position within somatropin. A high blood-brain barrier (BBB) influx was observed for $SDP_{101-121}$, while $SDP_{167-175}$ showed a negligible BBB influx. Based on the obtained results, the GHR binding of the selected SDPs is very low, requiring structural adaptations for further GHR-binding exploration.

Keywords: somatropin; cryptic peptides; GHR bioassay; native MS; tissue distribution; BBB distribution.

ABBREVIATIONS

hGH = human growth hormone

GHR = growth hormone receptor

IGF = insulin-like growth factor

hGHBp = human growth hormone binding protein

BBB = blood-brain barrier

ALS = amytrophic lateral sclerosis

SDPs = somatropin-derived peptides

TPCK = L-1-tosylamide-2-phenylethyl chloromethyl ketone

IDE = insulin degrading enzyme

PC1/2 = proprotein convertase1/2

hGHAb = human growth hormone antibody

TOF = time of flight

CTK = cytosolic tyrosine kinase

RMSD = root-mean square deviation

FA = formic acid

KH = Krebs-Henseleit

TFA = trifluoroacetic acid

ACN = acetonitrile

DMSO = dimethylsulfoxide

MRM = multiple reaction monitoring

EDC = N-ethyl-N'-(3-dimethylaminopropyl)carbodiimide

NHS = N-hydroxysuccinimide

BSA = bovine serum albumin

1. INTRODUCTION

The human growth hormone (hGH), secreted from the pituitary gland into the bloodstream, circulates through the entire body exerting several endocrine functions (regulation of growth, development, and metabolism of target tissues). It can also act as an autocrine or paracrine factor in many extrapituitary tissues (Harvey 2010). The hGH exerts its biological function directly by binding on the growth hormone receptor (GHR), which is ubiquitously distributed in the human body (Waters 2016), as well as indirectly through the induced production of insulin-like growth factor (IGF) 1 (Gunawardane et al. 2015). There is binding on two defined sites (*i.e.* site-I and site-II) on the GHR by at least four fragments within the hGH that represent the binding epitope: for site I, these are residues 41 – 68 and residues 167 – 175; for site II, these are residues 1 - 16 and residues 103 – 119 (Clackson and Wells 1995; Cunningham and Wells 1993; Sundström et al. 1996; De Vos, Ultsch, and Kossiakoff 1992). Binding on both sites is essential for dimerization which results in activation of the associated JAK2 and Src family kinases (De Palo et al. 2006; Waters 2016; Wells 1996).

Somatropin (recombinant prepared hGH) as GHR agonist and pegvisomant (GHR antagonist) were developed for the treatment of pathologies like growth hormone deficiency syndrome and acromegaly, interfering with the growth of children and adults, emerged (Gunawardane et al. 2015; Ayuk and Sheppard 2006; Tritos and Biller 2017). Due to the complex and multiple actions of hGH in target tissues and the involvement of the GHR, hGHBp, and IGF 1, also other diseases and conditions can be associated to the hGH, like chronic liver disease or cirrhosis (Wallace et al. 2002; ClinicalTrials.gov 2018; Mahesh and Kaskel 2008). Human growth hormone has also beneficial effects on memory, alertness, working capacity, and motivation. This indicates that hGH crosses the blood-brain barrier (BBB), acting on the central nervous system (Nyberg 2000; Bracke et al. 2018; Pan et al. 2005). In amyotrophic lateral sclerosis (ALS), GH insufficiency is observed, giving GH treatment the opportunity to be helpful due to its neuroprotective effects (Chung et al. 2015). Moreover, there is increasing evidence that the growth hormone receptor is overexpressed in several cancers (e.g. lung, pancreas, breast, skin) (Chhabra et al. 2018; Subramani et al. 2014; Gebre-Medhin et al. 2001; Sustarsic, Junnila, and Kopchick 2013). As such, the growth hormone and its receptor become potential targets in the diagnosis and treatment of these neurological diseases and cancers.

Different isoforms of the hGH as a result of heterogeneity at the level of the growth hormone gene and due to posttranscriptional processing (Waters 2016; Gunawardane et al. 2015), natural occurring metabolites, fragments, and segments are well-known, including their interaction with biological targets such as the GHR (De

Palo et al. 2006; De Vos, Ultsch, and Kossiakoff 1992; Wells 1996). Cryptic peptides can be classified into 3 groups (Autelitano et al. 2006), with the third group being peptides not endogenously expanded from their protein precursor, with a different or similar activity as their precursor. Therefore, due to the peptide advantages compared to proteins (Khanna 2012; Vlieghe et al. 2010), we explored the potential of some cryptic somatropin-derived peptides (SDPs) as therapeutic/diagnostic compounds.

First, an autodock simulation of the SDPs to the GHR was done to assess the binding potential and to make an appropriate selection of the SDPs. Furthermore, the novelty of the SDPs was demonstrated by *in silico* and *in vitro* enzymatic somatropin digests. The second part of the study focussed on the biological activity of the selected SDPs. The human growth hormone binding protein (hGHBp) and GHR binding capacity and tissue distribution (including BBB transport) were characterised.

2. MATERIALS AND METHODS

2.1 Chemicals, reagents, and equipment

Zomacton® 4 mg (Ferring, somatropin) was obtained from the University Hospital (Ghent, Belgium), hGHBp from MyBiosource (San Diego, USA), the SDPs (***Table 1***) from China Peptides (Shanghai, China), and dermorphin from Hanhong (Shanghai, China). The synthetically prepared SDPs were analysed for identity and purity (***SI 1***). The enzymes for peptide mapping, L-1-tosylamide-2-phenylethyl chloromethyl ketone (TPCK)-treated trypsin solution, immobilised chymotrypsin solution, and S. *aureus* V8 protease were purchased at Pierce (Erembodegem, Belgium) and Sigma Aldrich (Diegem, Belgium). Insulin degrading enzyme (IDE), proprotein convertase 1 (PC1), and proprotein convertase 2 (PC2) were from R&D systems (Minneapolis, USA). PD-10 sephadex G-25 M columns were acquired from GE Healthcare (Diegem, Belgium). Water was purified in-house using an Arium Pro VF TOC purification system (Sartorius, Göttingen, Germany), yielding 18.2 MΩ*cm and ≤ 5 ppb TOC quality water. Other chemicals and solvents were purchased from Merck (Overijse, Belgium), Sigma Aldrich (Diegem, Belgium), Biosolve (Valkenswaard, The Netherlands) or Fisher Scientific (Erembodegem, Belgium), all high quality (> 98% purity) and/or HPLC/MS grade. The human growth hormone antibody (hGHAb) was purchased at Fisher Scientific (Erembodegem, Belgium). The iodine-125 carrier free radionuclide was from Perkin Elmer (Zaventem, Belgium).

Table 1: Selected somatropin-derived peptides.

Peptide	Sequence	Position within somatropin		Binding site	Molecular weight (Da)	pI
SDP_{39-70}	NH_2-EQKYSFLQNPQTSLCFSESIP TPSNREETQQK-COOH	39-70	Loop between helix 1 and 2		3746.0	4.6
$SDP_{167-175}$	NH_2-RKDMDKVET-COOH	167-175	*C*-terminal part helix 4	Site I	1121.2	6.5
$SDP_{165/177}$	NH_2-CFRKDMDKVETFL-COOH	165-177	*C*-terminal part helix 4		1631.9	6.5
SDP_{1-18}	NH_2-FPTIPLSRLFDNAMLRAH-COOH	1-18	*N*-terminal part Helix 1		2099.4	10.5
SDP_{M+1-18}	NH_2-MFPTIPLSRLFDNAMLRAH-COOH	M+1-18	*N*-terminal part Helix 1	Site II	2230.6	10.5
$SDP_{101-121}$	NH_2-LVYGASDSNVYDLLKDLEEGI-COOH	101-121	Helix 3		2313.5	3.6

Somatropin proteolytic digest analysis and identification of SDP metabolites was performed using a HPLC-UV-MS apparatus consisting of a Spectra System separations module, a Finnigan LCQ Classic ion trap mass spectrometer in positive ion mode (all Thermo, San José, CA, USA) equipped with a Waters 2487 dual wavelength absorbance UV detector (Waters, Milford, USA) and Xcalibar 2.0 software (Thermo, San José, CA, USA) for data acquisition, as well as Thermo BioWorks software (San José, CA, USA) for protein identification. The purity analysis and *in vitro* metabolisation study was conducted on a HPLC-UV system equipped with a Waters Alliance 2695 separation module and a Waters 2996 PDA detector, with Empower 3 software for data handling (Waters, Milford, USA). The metabolisation study of $SDP_{1-18,M+1-18,101-121}$ in serum was conducted on a U(H)PLC system directly coupled to a Waters Xevo TQ-S detector (both from Waters, Milford, USA), while $SDP_{39-70,167-175,165-177}$ in serum was analysed with HPLC-UV system described above. Native MS studies were conducted on a Waters Synapt G2-Si high-resolution quadrupole time of flight (TOF) mass spectrometer (Waltham, MA) equipped with a LockSpray dual electrospray ion source. The PathHunter Cytosolic Tyrosine Kinase (CTK) assay with JAK2 target was from DiscoverX (Fremont, USA).

2.2 Autodock simulations

Docking simulations were performed using AutoDock 4.2, release 4.2.3 (Morris et al. 2009). Different variations of position, global orientation, and conformation of the ligand (here the peptide/somatropin fragment) were simulated in search for plausible binding places in the protein target binding site (the extracellular part of the GHR). Bond lengths, angles, and the backbone of the peptide were kept rigid to limit the numbers of freedom. Only torsion angles in the peptide side chains were flexible. Rigid body docking was done, in which no degrees of freedom were allowed in the hGHBp target. The full conformational space was then sampled stochastically and interesting peptide conformations (‘poses’) were located by a genetic algorithm followed by a local refinement,

based on an empirical free energy scoring function (Morris et al. 2009). The generated docked peptide-poses were then clustered on structural similarity, as measured by distance (root-mean square deviation (RMSD)) between poses. Highly populated clusters and clusters with low energy conformations were indicated as possible 'hits' and considered further.

2.3 *In silico* somatropin digestion

The SitePrediction webtool (http://www.dmbr.ugent.be/prx/bioit2-public/SitePrediction/) was used to explore proteolytic cleavage sites in the GH substrate (Verspurten et al. 2009; Rawlings, Tolle, and Barrett 2004). Cleavage sites with > 95% specificity were reported.

2.4 *In vitro* proteolytic digestions of somatropin

The novelty of the selected SDPs was confirmed by proteolytic digestion (S-carboxymethylation of cysteine residues) of somatropin by trypsin, chymotrypsin, S. *aureus* V8 protease, PC1, PC2, and IDE were used following the method as previously reported in (Bracke et al. 2014). Digestion was performed at 37°C while gently shaking at 300 rpm for the defined period of time in a thermomixer comfort (Eppendorf, Hamburg, Germany). One hundred microliter samples were taken after 0 h, 4 h, 24 h, 48 h and the reaction was stopped by addition of 20 µL formic acid (FA) to each sample. The samples were analysed by LC-MS as described in the peptide mapping section of reference (Bracke et al. 2014).

2.5 Metabolisation of the SDPs

The *in vitro* stability of the six SDPs was determined in serum, liver tissue homogenate, kidney tissue homogenate, and brain tissue homogenate according to standard protocols (Vergote et al. 2008; Svenson et al. 2010). The protein content of each homogenate was determined using the Pierce Modified Lowry Protein Assay method (Thermo Scientific) to generate a stock solution with a protein concentration of 0.6 mg/mL by dilution in Krebs-Henseleit buffer (KH) (pH 7.4, Sigma Aldrich). Briefly, 150 µL of a 1 mg/mL peptide solution, dissolved in KH buffer (pH 7.4) was added to 500 µL serum or tissue homogenate and incubated at 37°C while shaking at 750 rpm. Aliquots of 100 µL were sampled after 0, 15, 30, 60, and 120 minutes of incubation into tubes containing an equal volume of trifluoroacetic acid (TFA) (1% V/V) in acetonitrile (ACN) and immediately subjected to 95°C for 5 min, followed by flash cooling in an ice bath for 30 min. Finally, the samples were centrifuged at 20 000 g for 5 min at 5°C prior to HPLC-UV (tissue homogenates of all SDPs and serum of $SDP_{39\text{-}70}$, $SDP_{167\text{-}175}$, $SDP_{165\text{-}177}$) or

U(H)PLC-MRM (serum of SDP_{1-18}, $SDP_{M+1-18,}$ $SDP_{101-121}$) analysis. Blank control solutions were prepared as described above, without addition of peptide.

The half-life was determined as:

$$t_{1/2} = -\frac{\ln(2)}{slope} \qquad (1)$$

with the slope derived from the curve of the natural logarithm of the percentage of the amount at the start of the incubation, *i.e.* t = 0 min, versus time.

Because of our interest in the passage through the BBB (see further), the formed metabolites during incubation of the peptides in serum or brain homogenate were identified. Time points were chosen between approximately one or two half-lives as determined in the kinetic evaluation. In case of a half-life of > 120 minutes, $t_{120\ min}$ was chosen as time point for metabolite identification.

2.5.1 HPLC-UV analysis

The SDPs in tissue homogenates and $SDP_{39-70,167-175,165-177}$ in serum were separated on a Vydac Everest C_{18} column (4.6 x 250 mm, 5 µm) with suitable guard column (Grace, Lokeren, Belgium). The column was thermostated at a temperature of ± 40°C. The injection volume was 20 µL, the flow was 1 mL/min. Mobile phase A consisted out of 0.1% (V/V) TFA in 95/5 (V/V) H_2O/ACN, mobile phase B consisted out of 0.1% (V/V) TFA in 5/95 (V/V)) H_2O/ACN. The linear gradient program started with a 2 min isocratic hold at 100% A, followed by a linear gradient to 60% A and 40% B at 32 min. The column was rinsed with 100% B, followed by returning to the initial conditions and re-equilibration, giving a total run time of 50 min. UV detection was performed from 190 nm to 400 nm, with quantification at 210 nm.

2.5.2 U(H)PLC-MRM analysis

Sample preparation: the peptides $SDP_{1-18,M+1-18,101-121}$ were analysed simultaneously, *i.e.* in the same serum sample. The *in vitro* metabolisation was performed as described in 2.5 (materials and methods), with sampling adapted to 100 µL of sample added to 300 µL ACN and 0.1% TFA. Prior to injection, the samples were diluted in a novel anti-absorption diluent (BE2017/0040) to prevent adsorption to glass vials, by diluting 12 µL supernatant ad 2.0 mL diluent (*i.e.* 100 ng/mL).

U(H)PLC-MRM mass spectrometry method: a 2.1 x 100 mm reverse phase column (Waters, Acquity UPLC BEH C18, 1.7 µm) maintained at 45 ± 5°C was used for separation by a U(H)PLC system directly coupled to a Waters

Xevo TQ-S detector. A 2.0 µL sample was injected at a flow rate of 0.5 mL/min. The gradient program was as follows (A: 90/5/5 H_2O/ACN/DMSO (dimethylsulfoxide) containing 0.1% (m/V) FA and B: 5/90/5 H_2O/ACN/DMSO containing 0.1% (m/V) FA): isocratic phase of 100% A was maintained for 1.5 min, followed by a linear gradient over 5 min to 40% A (V/V) + 60% B (V/V). After the elution at 6.5 min, the column was washed with a 100% B flush and reverted to the initial state. The run was terminated after 15 min. The MS unit was operated in electrospray positive ionisation mode. Nitrogen was used as the nebulising gas and argon as the collision gas. Instrument settings were as follows: source and desolvation temperature, 500°C each; cone and desolvation gas flow, 150 and 1000 L/h resp. Acquisition was performed in the multiple reaction monitoring (MRM) mode and monitored from 1.5 min to 6.5 min (< 1.5 min and > 6.5 min to waste). Cone and capillary voltage, collision energy and mass transitions are given in ***Table 2***. Data were acquired using MassLynx software (V4.1 SCN 843, Waters, Milford, MA, USA).

Table 2: MRM transitions and parameters.

Parameter	SDP_{1-18}	SDP_{M+1-18}	$SDP_{101-121}$
MRM	700.67 > 821.08	744.32 > 651.44	1157.41 > 803.26
Capillary voltage (kV)	2.0	3.0	2.5
Cone voltage (V)	45	32	25
Collision energy (eV)	20	20	37

2.6 Native MS

The native MS method was essentially similar as previously described (Bracke et al. 2017): the non-denaturing MS data of standards (*i.e.* single peptides/proteins: all SDPs and hGHBp) and complex samples (*i.e.* a mixture of all six SDPs and hGHBp) were acquired in positive mode (ESI^+). A concentration of 666 nM for SDPs and 365 nM for hGHBp, dissolved in 25 mM ammonium acetate solution (pH 6.8 - 7.0) was used. Standards and samples were injected (10 µL) at a flow rate of 10 µL/min. The conditions of analysis were as follows: the source temperature was set at 150°C, desolvation gas temperature was 300°C, cone gas flow was 150 L/h, desolvation gas flow was 800 L/h, capillary voltage was 2.5 kV, and sampling cone voltage was 50.0 kV. Data were acquired between a m/z of 500 and 5000 Da.

2.7 *In vitro* GHR bio-assay

The PathHunter Cytosolic Tyrosine Kinase (CTK) Functional Assay (JAK2 target) was used for the profiling of the SDPs in agonist and antagonist format (Bracke et al. 2017). The cells were seeded in a total volume of 20 µL

Cell Plating Reagent into 384-well microplates. For agonist determination, cells were incubated with the peptides to induce a response. A 10 µM stock solution of each peptide was 5 times diluted in assay buffer to generate an intermediate solution. 5 µL of this intermediate dilution was added to each well and incubated for 3 h. In antagonist mode, cells were pre-incubated with peptide for 60 min at 37°C, followed by hGH agonist (EC_{80} challenge, 0.012 µg/mL hGH) incubation for 3 h. For the peptides, a concentration range between 0.5 nM – 10 µM was evaluated. Assay signal was generated through a single addition of 12.5 or 15 µL (50% V/V) of PathHunter Detection reagent cocktail for agonist and antagonist assays resp., followed by 1 h incubation at room temperature.

2.8 *In vivo* tissue distribution and the blood-brain barrier permeability

Female, Institute for Cancer Research, Caesarean Derived-1 (ICR-CD-1) mice of age 7 – 10 weeks and weighing 23 – 32 g, were obtained from Envigo RMSB.V. (Venray, The Netherlands). The animal experiments were approved by our institute (Ghent University, Faculty of Veterinary Medicine, approval number EC2014/128). Experiments were performed according to the Ethical Committee principles of laboratory animal welfare.

The radiolabelling of $SDP_{167-175}$ and $SDP_{101-121}$ is described in the supplementary information (***SI 2***).

Multiple time regression analysis and capillary depletion were performed as described by Bracke *et al.* (Bracke et al. 2018).

2.9 Statistics

Regression lines were computed using the least squares method. Regression lines were statistically compared using Prism 5 software (Graphpad, La Jolla, USA).

3. RESULTS

3.1 Selection of somatropin-derived peptides

Docking simulations were performed for each of the four core peptide fragments (corresponding to the four fragments of the hGH that constitute the binding epitope) to the extracellular part of the receptor. In these docking simulations, relying on a genetic and local search algorithm, global position and orientation of the peptide, as well as side chain conformations were exhaustively sampled in search for a peptide pose with optimal binding position on the GHR (***Figure 1***).

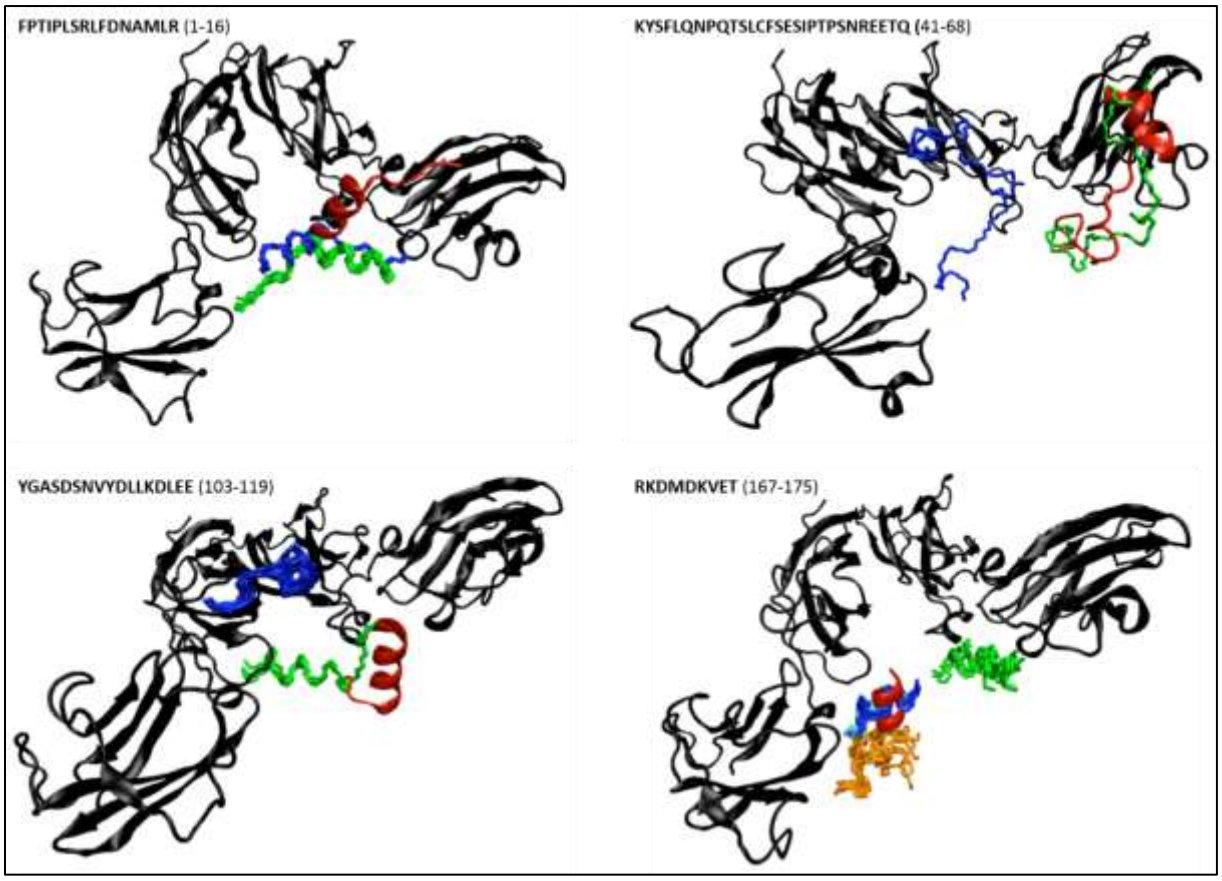

Figure 1: Docking simulation results of the core peptide fragments to the GHR. Black: extracellular part of GHR; red: location and conformation of the full peptide as determined in the crystal structure (PDB: 3HHR); blue, cyan, orange and green: prototypical peptide poses for highly populated clusters, or for clusters with the lowest mean binding energy.

The docking simulations predicted only favourable binding potential to the GHR for peptide 167-175. All other peptides were predicted to have unfavourable, positive binding energies with the GHR. In addition, peptides 1 – 16 and 103 – 119 interact mostly with the GHR in another location than the active site-I or –II. No meaningful clustering of poses was obtained from the ensemble of structures generated by docking simulations on peptide 41 – 68, thus *in silico*, this peptide did not interact with the receptor. For peptide 167 – 175, on the other hand, several clusters were successfully identified in the ensemble of the simulated docking poses. The poses had negative, favourable binding energies going from -1 to -3 kcal/mole and bounded either one of the symmetry-equivalent protein active sites. This peptide has *in silico* binding potential to the GHR.

Each peptide which represented the binding interface to the receptor, was selected with additionally one or two amino acids (based on the somatropin sequence) to the left and right of the fragment to offer the "core" more structural integrity and protection against exopeptidases (***Table 1***). For the N-terminal fragment (SDP_{1-18}), an additional N-terminal methionine was included (SDP_{M+1-18}). For fragment 167 - 175, which was predicted as most promising peptide binder, we selected the sequence as such ($SDP_{167-175}$) and with additional residues on the left and the right ($SDP_{165-177}$). $SDP_{101-121}$ represents residues 103 – 119 with two additional amino acids on both ends.

The selected peptides were verified for their novelty. The proteolytic digestions of somatropin with trypsin, chymotrypsin, S. *aureus* V8, IDE, PC1, and PC2 did not generate the proposed SDPs as metabolites. Moreover, *in silico* proteolytic digest by protease/peptidase enzymes (Werle and Bernkop-Schnürch 2006) on the somatropin sequence was performed, resulting in many possible predicted cleavage sites (***Figure 2***). Cleavage hotspots, here defined as more than three potential cleavage sites for a potential peptide bond, were R8-L9, R19-L20, Q22-L23, C33-A34, Q40-K41, R77-I78, R94-S95, K115-D116, R127-L128, R134-T135, R178-I179, and R183-S184.

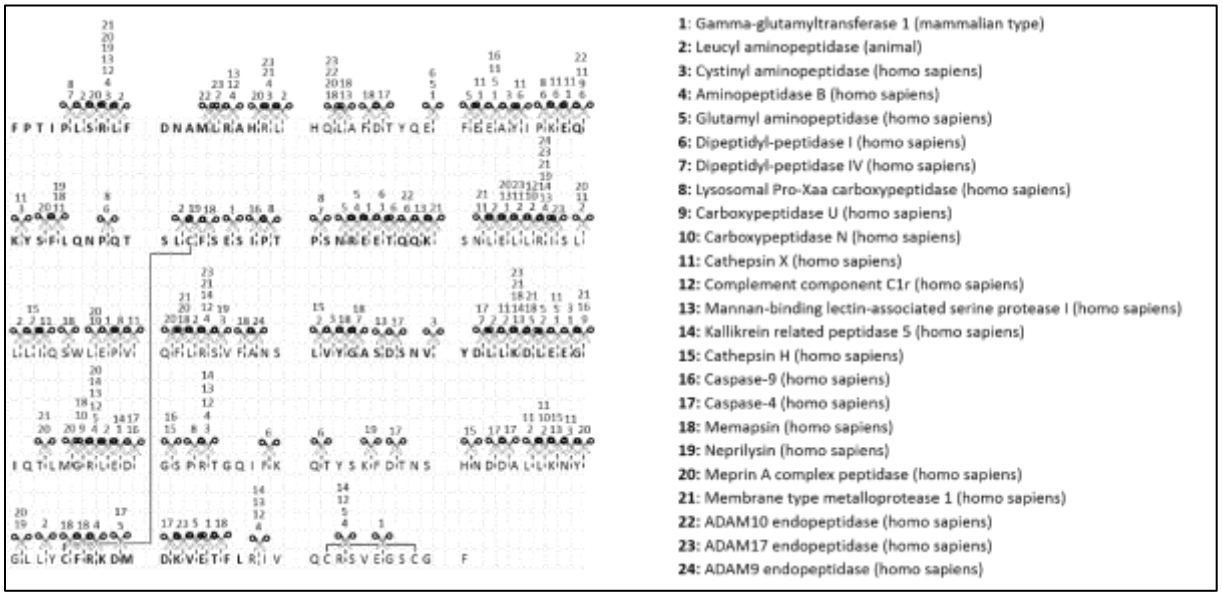

Figure 2: In silico cleavage site prediction on GH from typical proteases/peptidases in blood, kidney, and liver.

These cleavage hotspots, together with the GH-cleavage hotspots reported in literature show that the selected peptides are not likely to be metabolites from somatropin, emphasizing their novelty.

The six selected peptides were controlled for their identity and purity (***SI 1***). MS and MS^2 spectra confirmed the identity of the SDPs. All SDPs were found to have a purity of 95% or more except for $SDP_{39\text{-}70}$.

3.2 Metabolisation of the SDPs

The *in vitro* metabolisation was investigated in brain, liver, and kidney tissue homogenates, as well as in mouse serum (Vergote et al. 2008; Werle and Bernkop-Schnürch 2006). $SDP_{1\text{-}18,M+1\text{-}18,101\text{-}121}$ co-eluted with serum bulk components, which made the quantification using UV (at 210 nm) unreliable. For these 3 peptides in serum matrix, a MRM mass spectroscopic method was used. Further identification of the metabolites was performed to confirm the stability of the core of the SDPs. The analytical recovery was always above 90% (see ***SI 3***).

3.2.1 Metabolisation kinetics

In general, a peptide is considered stable if more than 90% of the original peptide is found at the time point of 120 min relative to $t_{0\ min}$ for serum or a tissue homogenate. In that case, the minimum half-life was calculated using the 90% value considering a first-order kinetic. The half-lives of the SDPs are presented in ***Table 3.***

Table 3: Metabolic half-lives for all SDPs in different mouse tissues.

Tissue	Half-life (min)					
	SDP_{39-70}	**$SDP_{167-175}$**	**$SDP_{165-177}$**	**SDP_{1-18}**	**SDP_{M+1-18}**	**$SDP_{101-121}$**
Brain	145.26	> 789	> 789	> 789	438.50	> 789
Liver	92.27	> 789	169.40	155.48	172.30	549.73
Kidney	22.52	48.57	13.88	9.12	12.43	44.98
Serum	72.48	113.27	89.10	20.74	17.86	> 789

The half-lives in mouse brain homogenate ranged from 2.42 h for SDP_{39-70} and 7.31 h for SDP_{M+1-18}, to more than 13 h for $SDP_{167-175}$, $SDP_{165-177}$, SDP_{1-18}, and $SDP_{101-121}$. Comparable values were seen in mouse liver homogenate. For the kidney homogenate, the peptides were less stable with half-lives ranging between 9.12 and 48.57 minutes. In the kidney, many peptides are filtered by the glomerulus, degraded and excreted. Also for GH, the kidney is the main excretion site (Rigamonti et al. 2012). For serum, $SDP_{101-121}$ had a half-life of more than 13 h, while the half-life of the other five SDPs was shorter (***Table 3***).

3.2.2 Identification of metabolites

For serum and brain, the metabolites were further identified to verify the stability of the receptor interaction "hotspots". Identified metabolites are given in ***Table 4***, with the parent peptide in bold and the major metabolite underlined. $SDP_{101-121}$ was stable: no metabolites were detected after 2 hours confirming the high stability in brain and serum as already observed in the kinetic evaluation. SDP_{39-70} has a major cleavage site at the peptide bond before and after F54 (*i.e.* the amino acid at position 54 within somatropin, ***Table 1***), which was not a known cleavage site based on the *in silico* data and literature. The other SDPs contain several cleavage sites in their sequence. The major cleavage site for $SDP_{167-175}$ and $SDP_{165-177}$ is the same: after the first lysine residue.

Table 4: Metabolites in mouse serum and brain tissue homogenate.

Peptide	RT (min)	Metabolite ID[1,2]	Tissue
SDP_{39-70}	15.99	FSESIPTPSNREETQQ	Serum
	19.53	EQKYSFLQNPQTSLCF	Serum & brain
	19.96	**EQKYSFLQNPQTSLCFSESIPTPSNREETQQK**	Brain
$SDP_{167-175}$	15.91	DKVET	Serum & brain
	16.76	**RKDMDKVET**	Serum & brain
	17.53	KDMDKVET	Serum & brain
	18.05	MDKVET	Serum
	18.88	DMDKVET	Serum
$SDP_{165-177}$	12.25	DMDKVET	Serum
	12.73	FRKDMDKVET	Serum
	17.82	KVETFL	Brain
	18.14	FRKDMDKVETFL	Serum & brain
	18.30	KDMDKVETFL	Brain
	19.99	**CFRKDMDKVETFL**	Serum & brain
	20.98	DMDKVETFL	Serum
SDP_{1-18}	20.59	IPLSRLFDNAMLRAH	Serum
	21.44	TIPLSRLFDNAMLRAH	Serum & brain
	22.18	TIPLSRLFDNAMLR	Serum
	23.01	PLSRLFDNAMLRAH	Serum & brain
	23.06	**FPTIPLSRLFDNAMLRAH**	Serum & brain
	23.74	FPTIPLSRLFDN	Brain
	24.09	FPTIPLSRLFDNA	Brain
	24.20	FPTIPLSRLFD	Brain
	26.03	FPTIPLSRLFDNAML	Brain
	76.50	FPTIPL	Serum
SDP_{M+1-18}	21.65	TIPLSRLFDNAMLRAH	Serum
	23.59	PLSRLFDNAMLRAH	Serum & brain
	23.59	PTIPLSRLFDNAMLRAH	Serum & brain
	23.64	**MFPTIPLSRLFDNAMLRAH**	Serum & brain
	24.60	MFPTIPLSRLFDN	Brain
	24.99	MFPTIPLSRLFDNA	Brain
	25.01	MFPTIPLSRLFD	Brain
$SDP_{101-121}$	**27.10**	**LVYGASDSNVYDLLKDLEEGI**	Serum & brain

[1] Bold: parent peptide, underlined: major metabolite in serum.

[2] Reporting threshold of 0.5% relative abundancy was applicable.

3.3 GH Receptor binding study of selected somatropin-derived peptides

3.3.1 Bioassay

The PathHunter Cytosolic Tyrosine Kinase (CTK) functional GHR bioassay was used to evaluate the functionality of the six SDPs for binding the human GHR and for activating/inhibiting the signal transduction cascade (SDP concentrations between 0.5 nM and 10 µM). Based on the dose response curves (***Figure 3***), none of the SDPs showed biological activity at a concentration of 10 µM or lower compared to the positive control, *i.e.* human GH for agonist mode and INCB018424 in antagonist mode being a potent, selective inhibitor of JAK1 and JAK2. The positive controls were given the maximum activity which can be reached and were set equal to 100%. It is thus concluded that there is no significant formation of a functional receptor dimer for JAK2 signaling (full agonist) or inhibition of functional receptor dimerization (full antagonist) under the applied conditions.

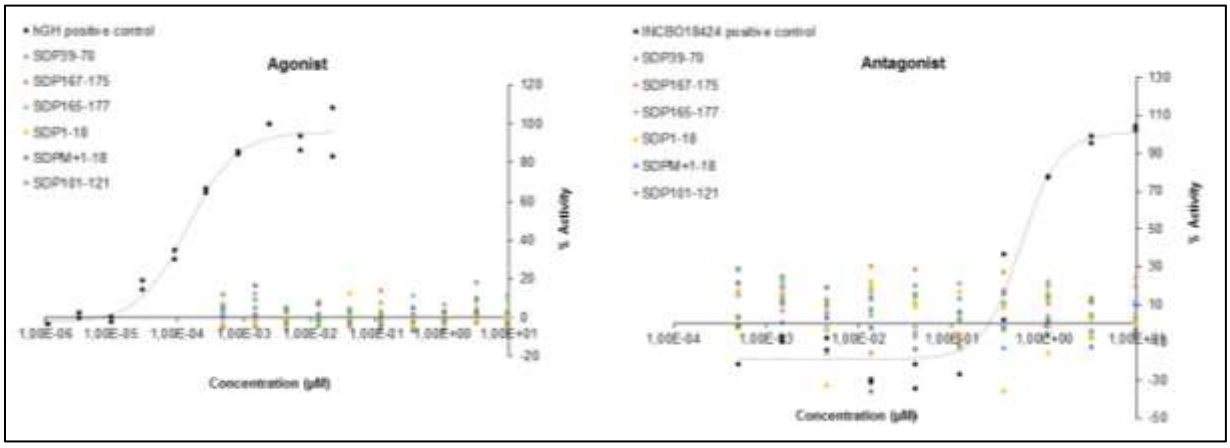

Figure 3: Dose response curves (DRC) of the hGHR bioassay in agonist (left) and antagonist (right) format.

3.3.2 Native MS

The molecular interaction of the SDPs to the hGHBp was further investigated using native MS. Native MS, also called non-denaturing MS, of the peptide, the receptor (*i.e.* hGHBp) and the peptide combined with the receptor mixture was used. The results are given in ***Figure 4.*** For all SDPs, no signals for a peptide:hGHBp complex were detected, as well as no significant decrease in free hGHBp responses (all still between 92% and 118%) was observed in the mixture samples compared to the single peptide/protein samples.

Additional binding experiments were performed with a surface acoustic wave biosensor towards the human growth hormone antibody (hGHAb) for further biological characterisation. The results are represented in ***SI 4***.

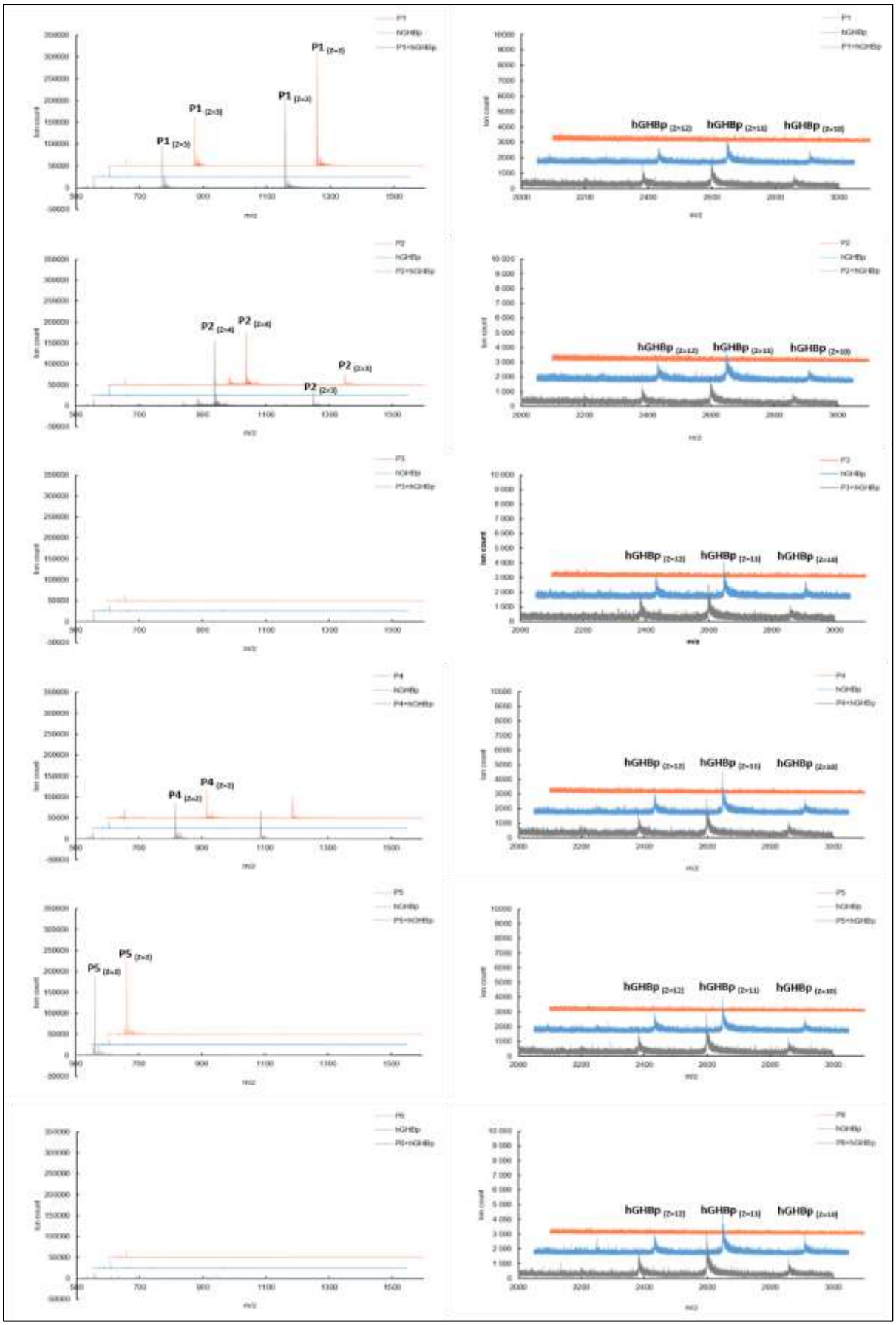

Figure 4: Overlay of typical native MS spectra from the functional SDP study. Left: m/z range from 500-1500, right: m/z range from 2000-3000. P1 = SDP_{39-70}, P2 = $SDP_{167-175}$, P3 = $SDP_{165-177}$, P4 = SDP_{1-18}, P5 = SDP_{M+1-18}, P6 = $SDP_{101-121}$.

3.4 Tissue distribution

The *in vivo* tissue distribution was evaluated for the two most metabolically stable SDPs. Therefore, the peptides were radiolabeled with ^{125}I (***SI 2***).

Figure 5 visualizes the tissue distribution of the radiolabeled peptides $SDP_{167-175}$ and $SDP_{101-121}$ at 15 min after injection. $SDP_{167-175}$ and $SDP_{101-121}$ are predominantly found in serum and in lesser extent in the kidney. The design of the blood-brain barrier is as such that almost no drugs or radiopharmaceuticals can enter in order to protect the brain against toxic agents (Pardridge 2012). However, $SDP_{167-175}$ and $SDP_{101-121}$ showed brain uptake.

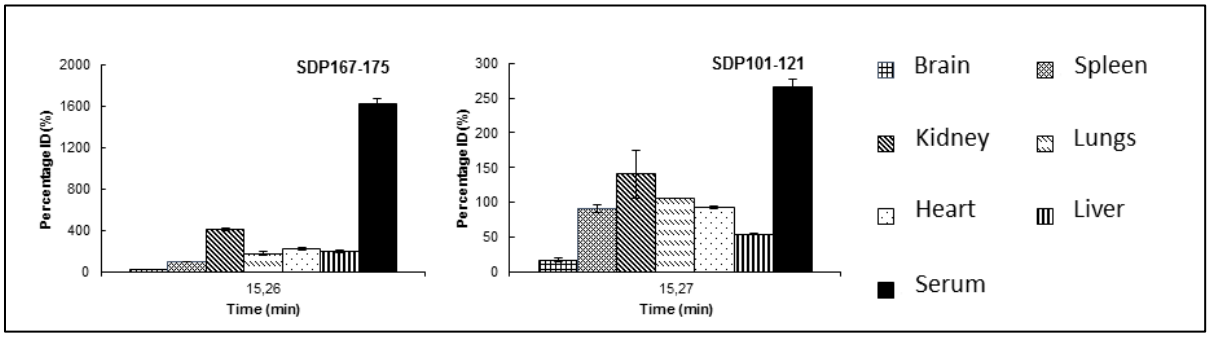

Figure 5: Tissue distribution at 15 minutes after IV-injection (mean ± SEM; n = 2).

Therefore, the brain tissue distribution of $SDP_{167-175}$ and $SDP_{101-121}$ was evaluated in more detail. A positive control (*i.e.* dermorphin) and a negative control (*i.e.* BSA) were included (Van Dorpe et al. 2012). $SDP_{101-121}$ showed a very pronounced influx with K_{in} = 1.43 µL/(g x min) (***Table 5, Figure 6***), which is significantly higher than somatropin and NOTA-modified somatropin (Bracke et al. 2018). The K_{in} value of $SDP_{167-175}$ was only 0.13 µL/(g x min). The initial distribution volume (V_i) of $SDP_{101-121}$ is 25 µL/g which is higher than the V_i of $SDP_{167-175}$ (*i.e.* 11 µL/g). Based on the peptide classification of Stalmans *et al.* (Stalmans et al. 2015), $SDP_{101-121}$ has a high influx while $SDP_{167-175}$ has a low influx and is not significantly different from BSA.

Table 5: Overview of the multiple time regression results (± SE).

Parameter	**$SDP_{167-175}$**	**$SDP_{101-121}$**	**BSA**	**Dermorphin**
K_{in} (µL/(g × min))	0.13 ± 0.10	1.43 ± 0.28	0.13 ± 0.05	0.48 ± 0.09
V_i (µL/g)	10.89 ± 1.17	25.41 ± 5.69	15.12 ± 0.69	18.24 ± 1.64

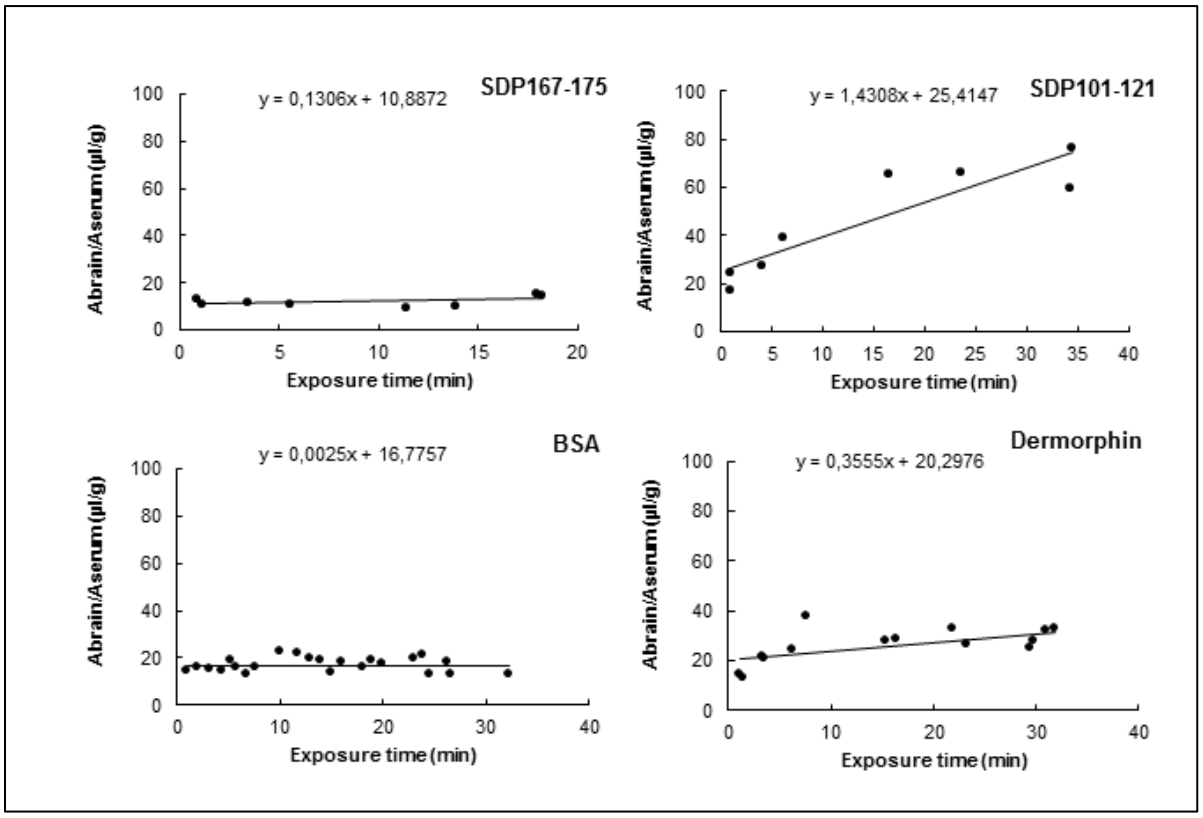

Figure 6: Linear regression curves of the exposure time versus the ratio of the brain and serum activity of the controls and peptides during the MTR experiments. BSA and dermorphin were evaluated as negative and positive controls.

4. DISCUSSION

Cryptic peptides can have bioactivities which are similar or totally different from their parent protein or prohormone (Autelitano et al. 2006; Baker et al. 2005). These cryptic peptides expand the medicinal landscape because smaller compounds with an activity depending on the need could be generated. In ***SI 5***, the currently known, natural, and smaller fragments of the hGH are listed, indicating the prohormone potential of the hGH and its receptor, the GHR. The selected somatropin-derived peptides (SDPs) are novel since they are not reported in literature or experimentally observed as metabolites. None of the SDPs resulted in an agonistic or antagonistic GHR cellular response under the selected conditions. To further evaluate binding of the SDPs on the receptor, native MS was conducted. The K_D of hGH for hGHBp (1:1 complex) is reported around 0.3 nM (Fuh et al. 1990). During the native MS study, concentrations of 666 nM SDP were used, identical to the concentrations used for somatropin in native MS (Bracke et al. 2017). At these SDP concentrations, no signals for a peptide:hGHBp complex were detected.

Chemical characterization and metabolic stability of the peptides under investigation was also performed. High purities of peptides are required for functionality studies, since impurities can lead to a biofunctional response leading to false positive or negative outcomes (Verbeken et al. 2012). All peptides had LC-based purities over

90%. Because no degradation peaks were observed and half-lives were longer than 15 minutes (except for the kidney), all peptides were considered as metabolically stable.

Investigation of the pharmacokinetics of the peptides through the blood-brain barrier (BBB) was performed because the BBB forms a barrier during the development of effective therapies targeting diseases in the central nervous system (CNS) (Pardridge 2005). $SDP_{101-121}$ (K_{in} of 1.43 µL/(g x min)) belongs to the group of peptides with a medium to high BBB influx according Stalmans classification (Stalmans et al. 2015). $SDP_{167-175}$ showed no significant influx compared to the vascular marker BSA, a protein which does not show BBB influx.

5. CONCLUSION

The aim of the study was to explore the potential of six somatropin-derived peptides (SDPs) as new diagnostic and/or therapeutic alternatives, selected based on the sequence which bind the site-I and site-II of the growth hormone receptor. The purity of the peptides was chemically characterised and found to be more than 95%, except for SDP_{39-70} (90% purity). The metabolic stability was evaluated looking at the recovery and appearance of degradation peaks. The possible metabolites and metabolisation kinetics in brain, kidney, liver, and serum was evaluated. In brain, liver tissue homogenates, and serum, all peptides were found stable ($t_{1/2}$ > 15 minutes). In kidney tissue homogenates, shorter half-lives were observed. For all SDPs, except $SDP_{101-121}$, metabolites were identified in serum and brain homogenates and the presence of different cleavage sites in the core sequence demonstrated. $SDP_{101-121}$ was extremely stable in the investigated tissues. A GHR bioassay and native MS was used to evaluate the functionality towards the GHR/GHBp binding; however, no binding of the SDPs was observed at the GHR or hGHBp. Two peptides ($SDP_{167-175}$ and $SDP_{101-121}$) were selected for tissue distribution, with $SDP_{101-121}$ showing a high BBB influx (K_{in} = 1.43 µL/(g x min)) and $SDP_{167-175}$ showing a very low BBB influx (K_{in} = 0.13 µL/(g x min)). Based on the results, adaption of the selected SDPs is required for further exploration in medical applications.

COMPLIANCE WITH ETHICAL STANDARDS

Funding: this research project was supported by grants from the Research Foundation FWO (Flanders) and NRF (South-Africa) (grant number G0G7617N) to Liesa Tack and from the Institute for the Promotion of Innovation through Science and Technology in Flanders (IWT-Vlaanderen) to Frederick Verbeke (Grant 131356).

Conflict of interests: Liesa Tack declares that she has no conflict of interests. Nathalie Bracke declares that she has no conflict of interests. Frederick Verbeke declares that he has no conflict of interests. Evelien Wynendaele

declares that she has no conflicts of interests. Ewald Pauwels declares that he has no conflict of interests. Alex Maes declares that he has no conflict of interest. Christophe Van de Wiele declares that he has no conflict of interests. Mike Sathekge declares that he has no conflict of interests. Bart De Spiegeleer declares that he has no conflict of interests.

Ethical approval: This article does not contain any studies with human participants or animals performed by any of the authors.

REFERENCES

Autelitano, Dominic J, Antonio Rajic, Ian A Smith, Michael C Berndt, Leodevico L Ilag, and Mathew Vadas. 2006. "The Cryptome: A Subset of the Proteome, Comprising Cryptic Peptides with Distinct Bioactivities." *Drug Discovery Today* 11 (7–8): 306–14. https://doi.org/10.1016/j.drudis.2006.02.003.

Ayuk, J, and MC Sheppard. 2006. "Growth Hormone and Its Disorders." *Postgraduate Medical Journal* 82 (963): 24–30. https://doi.org/10.1136/pgmj.2005.036087.

Baker, A. M., D. C. Batchelor, G. B. Thomas, J. Y. Wen, M. Rafiee, H. Lin, and J. Guan. 2005. "Central Penetration and Stability of N-Terminal Tripeptide of Insulin-like Growth Factor-I, Glycine-Proline-Glutamate in Adult Rat." *Neuropeptides* 39 (2): 81–87. https://doi.org/10.1016/j.npep.2004.11.001.

Bracke, Nathalie, Yorick Janssens, Evelien Wynendaele, Liesa Tack, Alex Maes, Christophe Van De Wiele, Mike Sathekge, and Bart De Spiegeleer. 2018. "BBB Transport of NOTA-Modified Proteins: The Somatropin Case." *The Quarterly Journal of Nuclear Medicine and Molecular Imaging*.

Bracke, Nathalie, Evelien Wynendaele, Matthias D'Hondt, Rob Haselberg, Govert W. Somsen, Ewald Pauwels, Christoph Van de Wiele, and Bart De Spiegeleer. 2014. "Analytical Characterization of NOTA-Modified Somatropins." *Journal of Pharmaceutical and Biomedical Analysis* 96. Elsevier B.V.: 1–9. https://doi.org/10.1016/j.jpba.2014.03.014.

Bracke, Nathalie, Han Yao, Evelien Wynendaele, Frederick Verbeke, Xiaolong Xu, Bert Gevaert, Alex Maes, et al. 2017. "In Vitro Functional Quality Characterization of NOTA-Modified Somatropins." *Analytical Chemistry* 89 (5): 2764–72. https://doi.org/10.1021/acs.analchem.6b03601.

Chhabra, Y., H. Y. Wong, L. F. Nikolajsen, H. Steinocher, A. Papadopulos, K. A. Tunny, F. A. Meunier, et al. 2018. "A Growth Hormone Receptor SNP Promotes Lung Cancer by Impairment of SOCS2-Mediated

Degradation." *Oncogene* 37 (4). Nature Publishing Group: 489–501. https://doi.org/10.1038/onc.2017.352.

Chung, JY, JS Sunwoo, MW Kim, and M Kim. 2015. "The Neuroprotective Effects of Human Growth Hormone as a Potential Treatment for Amytrophic Lateral Sclerosis." *Neural Regeneration Research* 10 (8): 1201–3.

Clackson, T, and JA Wells. 1995. "A Hot-Spot of Binding-Energy in a Hormone-Receptor Interface.Pdf." *Science* 267 (5196): 383–86.

ClinicalTrials.gov. 2018. "Growth Hormone Therapy in Liver Cirrhosis." US National Library of Medicine. 2018. https://clinicaltrials.gov/ct2/about-site/terms-conditions.

Cunningham, B C, and J A Wells. 1993. "Comparison of a Structural and a Functional Epitope." *Journal of Molecular Biology* 234 (3): 554–63. https://doi.org/10.1006/jmbi.1993.1611.

Dorpe, Sylvia Van, Antoon Bronselaer, Joachim Nielandt, Sofie Stalmans, Evelien Wynendaele, Kurt Audenaert, Christophe Van De Wiele, et al. 2012. *Brainpeps: The Blood-Brain Barrier Peptide Database*. *Brain Structure and Function*. Vol. 217. https://doi.org/10.1007/s00429-011-0375-0.

Fuh, G, MG Mulkerrin, S Bass, N MacFarland, M Brochier, JH Bourell, DR Light, and JA Wells. 1990. "The Human Growth Hormone Receptor. Secretion from Escherichia Coli and Disulfide Bonding Pattern of the Extracellular Binding Domain." *J. Biol. Chem.* 265 (6): 3111–15.

Gebre-Medhin, M, L G Kindblom, H Wennbo, J Törnell, and J M Meis-Kindblom. 2001. "Growth Hormone Receptor Is Expressed in Human Breast Cancer." *The American Journal of Pathology* 158 (4): 1217–22. https://doi.org/10.1016/S0002-9440(10)64071-0.

Gunawardane, K, TK Hansen, N Muller, JS Christiansen, and JOL Jorgensen. 2015. "Normal Physiology of Growth Hormone in Adults." In *Endotext*, edited by LJ De Groot, G Chrousos, K Dungan, and Et Al. South Dartmouth.

Harvey, S. 2010. "Extrapituitary Growth Hormone." *Endocrinology* 38 (3): 335–59. https://doi.org/10.1007/s12020-010-9403-8.

Khanna, Ish. 2012. "Drug Discovery in Pharmaceutical Industry: Productivity Challenges and Trends." *Drug Discovery Today* 17 (19–20). Elsevier Ltd: 1088–1102. https://doi.org/10.1016/j.drudis.2012.05.007.

Mahesh, Shefali, and Frederick Kaskel. 2008. "Growth Hormone Axis in Chronic Kidney Disease." *Pediatric Nephrology* 23 (1): 41–48. https://doi.org/10.1007/s00467-007-0527-x.

Morris, Gm, Ruth Huey, W Lindstrom, MF Sanner, RK Belew, DS Goodsell, and AJ Olson. 2009. "AutoDock4 and AutoDockTools4: Automated Docking with Selective Receptor Flexibility." *Journal of Computer Chemistry* 30 (16): 2785–91. https://doi.org/10.1002/jcc.21256.AutoDock4.

Nyberg, Fred. 2000. "Growth Hormone in the Brain: Characteristics of Specific Brain Targets for the Hormone and Their Functional Significance." *Frontiers in Neuroendocrinology* 21 (4): 330–48. https://doi.org/10.1006/frne.2000.0200.

Palo, Elio F. De, Vincenzo De Filippis, Rosalba Gatti, and Paolo Spinella. 2006. "Growth Hormone Isoforms and Segments/Fragments: Molecular Structure and Laboratory Measurement." *Clinica Chimica Acta* 364 (1–2): 67–76. https://doi.org/10.1016/j.cca.2005.06.009.

Pan, Weihong, Yongmei Yu, Courtney M. Cain, Fred Nyberg, Pierre O. Couraud, and Abba J. Kastin. 2005. "Permeation of Growth Hormone across the Blood-Brain Barrier." *Endocrinology* 146 (11): 4898–4904. https://doi.org/10.1210/en.2005-0587.

Pardridge, William M. 2005. "The Blood-Brain Barrier: Bottleneck in Brain Drug Development." *NeuroRx* 2 (1): 3–14. https://doi.org/10.1602/neurorx.2.1.3.

Pardridge, William M. 2012. "Drug Transport across the Blood-Brain Barrier." *Journal of Cerebral Blood Flow and Metabolism* 32 (11). Nature Publishing Group: 1959–72. https://doi.org/10.1038/jcbfm.2012.126.

Rawlings, Neil D., D. Tolle, and Alan J. Barrett. 2004. "MEROPS: The Peptidase Database." *Nucleic Acids Research* 32: D160–64. https://doi.org/10.1093/nar/27.1.325.

Rigamonti, A. E., M. Bozzola, G. Banfi, C. Meazza, E. E. Müller, and S. G. Cella. 2012. "Growth Hormone Variants: A Potential Avenue for a Better Diagnostic Characterization of Growth Hormone Deficiency in Children." *Journal of Endocrinological Investigation* 35 (10): 937–44. https://doi.org/10.3275/8647.

Stalmans, S., B. Gevaert, E. Wynendaele, J. Nielandt, G.D. Tré, K. Peremans, C. Burvenich, and B. De Spiegeleer. 2015. "Classification of Peptides According to Their Blood-Brain Barrier Influx." *Protein and Peptide Letters* 22 (9): 768–75. https://doi.org/10.2174/0929866522666150622101223.

Subramani, Ramadevi, Rebecca Lopez-Valdez, Alyssa Salcido, Thiyagarajan Boopalan, Arunkumar Arumugam, Sushmita Nandy, and Rajkumar Lakshmanaswamy. 2014. "Growth Hormone Receptor Inhibition Decreases the Growth and Metastasis of Pancreatic Ductal Adenocarcinoma." *Experimental & Molecular*

Medicine 46 (10). Nature Publishing Group: e117. https://doi.org/10.1038/emm.2014.61.

Sundström, Michael, Tomas Lundqvist, Joakim Rödin, Lutz B Giebel, Dan Milligan, and Gunnar Norstedt. 1996. "Crystal Structure of an Antagonist Mutant of Human Growth Hormone, G120R, in Complex with Its Receptor at 2.9 Å Resolution." *J. Biol. Chem.* 271 (50): 32197–203. https://doi.org/10.1074/jbc.271.50.32197.

Sustarsic, Elahu G., Riia K. Junnila, and John J. Kopchick. 2013. "Human Metastatic Melanoma Cell Lines Express High Levels of Growth Hormone Receptor and Respond to GH Treatment." *Biochemical and Biophysical Research Communications* 441 (1). Elsevier Inc.: 144–50. https://doi.org/10.1016/j.bbrc.2013.10.023.

Svenson, Johan, Valentijn Vergote, Rasmus Karstad, Christian Burvenich, John S Svendsen, Bart De Spiegeleer, and Bart De Spiegeleer. 2010. "Metabolic Fate of Lactoferricin-Based Antimicrobial Peptides: Effect of Truncation and Incorporation of Amino Acid Analogs on the in Vitro Metabolic Stability." *The Journal of Pharmacology and Experimental Therapeutics* 332 (3): 1032–39. https://doi.org/10.1124/jpet.109.162826.

Tritos, Nicholas A, and Beverly MK Biller. 2017. "Pegvisomant: A Growth Hormone Receptor Antagonist Used in the Treatment of Acromegaly." *Pituitary* 20 (1). Springer US: 129–35. https://doi.org/10.1007/s11102-016-0753-y.

Verbeken, Mathieu, Evelien Wynendaele, Romain A. Lefebvre, Els Goossens, and Bart De Spiegeleer. 2012. "The Influence of Peptide Impurity Profiles on Functional Tissue-Organ Bath Response: The 11-Mer Peptide INSL6[151-161] Case." *Analytical Biochemistry* 421 (2). Elsevier Inc.: 547–55. https://doi.org/10.1016/j.ab.2011.09.031.

Vergote, Valentijn, Sylvia Van Dorpe, Kathelijne Peremans, Christian Burvenich, and Bart De Spiegeleer. 2008. "In Vitro Metabolic Stability of Obestatin: Kinetics and Identification of Cleavage Products." *Peptides* 29 (10): 1740–48. https://doi.org/10.1016/j.peptides.2008.05.018.

Verspurten, Jelle, Kris Gevaert, Wim Declercq, and Peter Vandenabeele. 2009. "SitePredicting the Cleavage of Proteinase Substrates." *Trends in Biochemical Sciences* 34 (7): 319–23. https://doi.org/10.1016/j.tibs.2009.04.001.

Vlieghe, Patrick, Vincent Lisowski, Jean Martinez, and Michel Khrestchatisky. 2010. "Synthetic Therapeutic Peptides: Science and Market." *Drug Discovery Today* 15 (1–2): 40–56.

https://doi.org/10.1016/j.drudis.2009.10.009.

Vos, A. M. De, M. Ultsch, and A. A. Kossiakoff. 1992. “Human Growth Hormone and Extracellular Domain of Its Receptor: Crystal Structure of the Complex.” *Science* 255 (5042): 306–12.

Wallace, J D, W J Abbott-Johnson, D H Crawford, R Barnard, J M Potter, and R C Cuneo. 2002. “GH Treatment in Adults with Chronic Liver Disease: A Randomized, Double-Blind, Placebo-Controlled, Cross-over Study.” *Journal of Clinical Endocrinology & Metabolism* 87 (6): 2751–59. https://doi.org/10.1210/jc.87.6.2751.

Waters, Michael J. 2016. “The Growth Hormone Receptor.” *Growth Hormone and IGF Research* 28. Elsevier B.V.: 6–10. https://doi.org/10.1016/j.ghir.2015.06.001.

Wells, JA. 1996. “Binding in the Growth Hormone Receptor Complex.” *Proceedings of the National Academy of Sciences of the United States of America* 93 (1): 1–6. https://doi.org/10.1073/pnas.93.1.1.

Werle, M., and A. Bernkop-Schnürch. 2006. “Strategies to Improve Plasma Half Life Time of Peptide and Protein Drugs.” *Amino Acids* 30 (4): 351–67. https://doi.org/10.1007/s00726-005-0289-3.